JOURNAL OF TROPICAL PHARMACY AND CHEMISTRY
https://jtpc.ff.unmul.ac.id

Volume 10.2

Original Article

Statistical Modeling and Numerical Optimization of Ultrasound-Assisted Phenolic and Flavonoid Extraction from *Momordica charantia* Fruit

Tubagus Akmal*, Cszahreyloren Vitamia, Andi Ika Julianti Handayani

Bumi Siliwangi Pharmacy Academy, Bandung, 40286, West Java, Indonesia

*Corresponding author: tubagus.akmal93@gmail.com

Abstract

This study modeled ultrasound-assisted extraction (UAE) of total phenolic content (TPC) and total flavonoid content (TFC) from Momordica charantia fruit using a three-factor Box–Behnken design. Ethanol concentration (0–96%), liquid-to-solid ratio (10–40 mL/g), and extraction time (5–30 min) were evaluated at a fixed bath temperature of 50 °C. Box–Cox-guided square-root and $\log_{10}$ transformations were applied to TPC and TFC, respectively. The selected linear models were significant ($p < 0.0001$), with R^2/adjusted R^2/predicted R^2 of 0.9582/0.9469/0.9264 for TPC and 0.9129/0.8892/0.8148 for TFC. Liquid-to-solid ratio significantly affected TPC, whereas ethanol concentration and liquid-to-solid ratio significantly affected TFC; extraction time was not significant. TPC showed significant lack-of-fit ($p = 0.0426$), while TFC lack-of-fit was not significant ($p = 0.0636$). Joint numerical optimization predicted 95.994% ethanol, 40.000 mL/g, and 5.000 min (desirability = 0.955), with bias-corrected mean predictions of 109.054 mg GAE/g dry extract and 123.371 mg QE/g dry extract. This boundary solution was not experimentally confirmed. At a separate confirmation location (82.8208%, 37.4455 mL/g, 26.3205 min), TPC was substantially underpredicted, whereas TFC agreed more closely with the model. These findings identify a preliminary operating direction for UAE but indicate that the TPC model requires additional design points, stronger replication, and assay-specific verification before confirmatory or scale-up use.

Keywords: Box–Behnken design; *Momordica charantia*; numerical optimization; total flavonoid content; total phenolic content; ultrasound-assisted extraction

Accepted: 1 June 2026
Approved: 29 July 2026
Publication: 31 July 2026

Citation : T. Akmal, C. Vitamia, and A. I. J. Handayani, "Statistical Modeling and Numerical Optimization of Ultrasound-Assisted Phenolic and Flavonoid Extraction from Momordica charantia Fruit", Journal of Tropical Pharmacy and Chemistry, vol. 10, no. 2, pp. 64–72, Jul. 2026, doi: 10.30872/jtpc.v10i2.430

Doi: 10.30872/jtpc.v10i2.430

1 Introduction

Momordica charantia L., commonly known as bitter melon, has long been utilized in traditional medicine due to its wide spectrum of pharmacological properties, including antidiabetic, antioxidant, anti-inflammatory, and anticancer activities [1]-[3]. These biological effects are largely attributed to its rich content of secondary metabolites such as phenolics and flavonoids, which act as potent antioxidants and contribute to the therapeutic potential of the plant [4], [5]. Given the increasing global interest in functional foods and natural antioxidants, efficient extraction of bioactive compounds from *M. charantia* has become an important research focus [6].

Conventional extraction methods, such as maceration and reflux, are often limited by long extraction times, excessive solvent consumption, and relatively low extraction efficiency [7]. These drawbacks not only hinder process scalability but may also compromise the stability of sensitive phytochemicals [8]. In recent years, ultrasound-assisted extraction (UAE) has emerged as a promising alternative due to its ability to disrupt plant cell walls through acoustic cavitation, thereby enhancing solvent penetration, reducing processing time, and improving extraction yield [9]. Moreover, UAE is considered an environmentally friendly technology that aligns with the principles of green chemistry [10]. Despite its advantages, the efficiency of UAE strongly depends on multiple parameters, including solvent concentration, liquid–solid ratio, and extraction time [11]. Empirical optimization of these factors can be laborious and less reliable, highlighting the need for systematic approaches [12]. Response surface methodology (RSM) is widely employed to map factor–response relationships and to identify operating optima with a reduced number of experiments [13]. While UAE has been explored for various botanicals, to our knowledge few studies have jointly optimized total phenolic content (TPC) and total flavonoid content (TFC) from M. charantia using an ethanol–water system under a Box–Behnken design (BBD), followed by rigorous model selection and transformation to stabilize variance [14].

UAE optimization of bitter melon is not itself novel. Hani et al. used a three-factor Box–Behnken design (BBD) to study extraction time, temperature, and induced calorimetric power in fruit [15], whereas Lee and Yoon used a probe system and a central composite design to optimize ethanol concentration, ultrasonic power, and time at a fixed liquid-to-solid ratio [16]. In contrast, the present study evaluates a bath system and treats the liquid-to-solid ratio as an experimental factor, while simultaneously modeling TPC and TFC. The specific contribution is thus the comparison of transformed predictive models and their joint numerical optimization under this factor set, rather than a claim of being the first UAE/RSM study on *M. charantia*.

Accordingly, this study aimed to quantify the effects of ethanol concentration, liquid-to-solid ratio, and extraction time on TPC and TFC from *M. charantia* fruit, select parsimonious transformed models using predictive and diagnostic criteria, and identify a joint numerical optimum. Particular attention was given to the reliability limits of the TPC model, assay-related uncertainty, and the distinction between a model-predicted optimum and an experimentally confirmed condition.

2 Method

2.1 Materials

Fresh fruits of *Momordica charantia* L. were obtained from a local market in Bandung, West Java, Indonesia. The fruits were washed, sliced, dried at 45 °C until constant weight, and ground into fine powder. Analytical grade ethanol (96%), Folin–Ciocalteu reagent, sodium carbonate (Na_2CO_3), aluminum chloride ($AlCl_3$), sodium acetate (CH_3COONa), gallic acid, and quercetin standards were purchased from Merck (Germany). All other chemicals and solvents used were of analytical grade.

2.2 Ultrasound-assisted Extraction (UAE)

Extraction was conducted in a 2 L ultrasonic bath (EECOO, China) operated at a fixed nominal frequency of 40 kHz and rated power of 120 W. The ratio of rated power to bath capacity was therefore 60 W/L. This value is reported as nominal equipment power density; actual acoustic power delivered to

Doi: 10.30872/jtpc.v10i2.430

each sample was not determined calorimetrically and may differ because of bath loading, vessel geometry, sample position, coupling, and temperature [17], [18].

For each run, 1.0 g of dried powder was combined with the volume and ethanol–water composition specified by the experimental design. Samples were sonicated for the specified duration while the bath temperature was maintained at 50 °C. Temperature was fixed to restrict the design to three factors and to provide an intermediate condition between improved solvent transport at elevated temperature and the risk of thermal or sonochemical alteration. Previous bitter melon UAE studies have examined or fixed temperatures from approximately 40 to 60 °C [15], [16], the present choice should therefore be understood as a controlled operating condition, not an optimized temperature.

After sonication, the mixtures were filtered through Whatman No. 1 filter paper. The filtrates were centrifuged at 4500 rpm for 10 min, and the supernatants were evaporated at 40 °C in a vacuum oven. The dry extracts were stored at 4 °C until analysis [19].

2.3 Experimental Design using Box–Behnken Design

Optimization of UAE parameters was performed using a three-factor, three-level Box–Behnken Design (BBD). The independent variables were ethanol concentration (0-96, %), liquid–solid ratio (10-40, mL/g), and extraction time (5-30, min), each evaluated at low, medium, and high levels. A total of 15 experimental runs were generated including three replicates at the center point to estimate pure error. The experimental design and observed responses are summarized in Table 1. The responses measured were total phenolic content (TPC, mg GAE/g dry extract) and total flavonoid content (TFC, mg QE/g dry extract) [20], [21].

Table 1 Box behnken design of three variables with their observed responses of M. charantia extract

Run	Variables			Responses			
	A	B	C	TPC		TFC	
				Predicted	Observed	Predicted	Observed
1	48	25	17.5	46.85	58.59	38.80	41.74
2	48	40	5	108.66	120.78	87.56	68.54
3	96	10	17.5	11.46	10.44	25.34	17.14
4	0	40	17.5	106.18	91.06	59.43	61.21
5	0	25	5	48.48	47.7	30.18	34.26
6	48	25	17.5	46.85	58.33	38.80	38.81
7	48	25	17.5	46.85	54.77	38.80	37.01
8	96	25	30	45.25	45.44	49.88	66.52
9	0	25	30	45.23	43.58	26.33	28.48
10	0	10	17.5	11.45	9.59	13.37	14.04
11	96	40	17.5	106.21	84.44	112.57	125.29
12	48	10	5	12.27	9.29	19.71	18.39
13	48	40	30	103.76	110.04	76.40	57.25
14	48	10	30	10.67	9.95	17.19	17.42
15	96	25	5	48.50	48.89	57.17	75.57

A: ethanol concentration (%); B: liquid solid ratio (mL/g); C: extraction time (minutes); TPC: total phenolic content (mg GAE/g DE); TFC: total flavonoid content (mg QE/g DE). Predicted values are back-transformed medians.

2.4 Determination of Total Phenolic Content (TPC)

TPC was determined using the Folin–Ciocalteu method with slight modifications. Briefly, 0.5 mL of appropriately diluted extract was mixed with 2.5 mL of 10% Folin–Ciocalteu reagent and incubated for 5 min at room temperature. Then, 2.0 mL of 7.5% Na_2CO_3 solution was added and the mixture was incubated in the dark for 45 min. Absorbance was measured at 765 nm using a UV-Vis spectrophotometer

Doi: 10.30872/jtpc.v10i2.430

(Shimadzu UV-1780, Japan). Gallic acid was used to generate the calibration curve (10–320 µg/mL), and results were expressed as mg gallic acid equivalents (GAE) per g of dry extract [20].

2.5 Determination of Total Flavonoid Content (TFC)

TFC was measured using the aluminum chloride colorimetric method. Briefly, 1.0 mL of extract solution was mixed with 2.0 mL of 2% $AlCl_3$ in methanol and 3.0 mL of 5% sodium acetate solution. After incubation at room temperature for 30 min, absorbance was recorded at 415 nm. Quercetin was used as a standard (10–100 µg/mL), and results were expressed as mg quercetin equivalents (QE) per g of dry extract [21].

2.6 Statistical Analysis

Box–Cox diagnostics indicated square-root transformation for TPC ($\lambda = 0.5$; estimated optimum $\lambda = 0.59$, 95% CI 0.28–0.89) and base-10 logarithmic transformation for TFC ($\lambda = 0$; estimated optimum $\lambda = -0.01$, 95% CI −0.59–0.53). Linear, two-factor interaction, quadratic, and estimable higher-order models were compared using sequential p-values, lack-of-fit, adjusted R^2, predicted R^2, predicted residual sum of squares (PRESS), and residual/influence diagnostics. Cubic models were aliased. The selected models were linear on their respective transformed scales because added terms were not significant and reduced predicted R^2. This selection does not override the statistically significant TPC lack-of-fit, which is treated as a limitation [22].

Residual normality and predicted-versus-actual plots were examined, together with externally studentized residuals, Cook's distance, leverage, and DFFITS. An observation flagged by an influence statistic was retained unless a documented analytical or transcription error existed. Joint numerical optimization constrained A, B, and C to the tested ranges and assigned both TPC and TFC the goal "maximize," with equal importance (3). Back-transformed medians were obtained directly from the fitted equations. For reporting model-predicted means, the TPC median was corrected by adding the transformed-scale residual mean square (0.3798), and the TFC median was multiplied by $\exp\{0.5(\ln 10)^2(0.0087)\} = 1.0233$.

3 Result and Discussion

3.1 Model Fitting and Statistical Analysis

The observed TPC ranged from 9.29 to 120.78 mg GAE/g DE, and TFC ranged from 14.04 to 125.29 mg QE/g DE (Table 1). The linear models for $\sqrt{\text{TPC}}$ and $\log_{10}(\text{TFC})$ were both significant ($p < 0.0001$). Table 2 presents the ANOVA and fit statistics on the transformed scales.

Table 2 ANOVA and fit statistics for the selected transformed linear models

Source of variation	Regression Coefficient							
	TPC				TFC			
	Sum of squares	df	F-value	P-value	Sum of squares	df	F-value	P-value
Model	95.90	3	84.16	< 0.0001***	1.00	3	38.43	< 0.0001***
A (%)	4.408×10^{-6}	1	0.0000	0.9973	0.1539	1	17.74	0.0015**
B (ml/g)	95.78	1	252.17	< 0.0001***	0.8395	1	96.75	< 0.0001***
C (min)	0.1128	1	0.2969	0.5967 ns	0.0070	1	0.8116	0.3870 ns
Residual	4.18	11			0.0954	11		
Lack of fit	4.14	9	22.85	0.0426*	0.0941	9	15.10	0.0636ns
Pure error	0.0402	2			0.0014	2		
Total correction	100.07	14			1.10	14		
R^2	0.9582				0.9129			
R^2 Adjusted	0.9469				0.8892			
R^2 Predicted	0.9264				0.8148			
CV	9.00				5.86			

Doi: 10.30872/jtpc.v10i2.430

Adeq. Precision	22.49	19.2362
PRESS	7.37	0.2030

A = ethanol concentration (%); B = liquid–solid ratio (mL/g); C = extraction time (min). Significance codes: *** $p < 0.001$; ** $p < 0.01$; * $p < 0.05$; ns $p \geq 0.05$. CV, coefficient of variation; PRESS, predicted residual sum of squares. ANOVA was performed on $\sqrt{\text{TPC}}$ and $\log_{10}$(TFC).

For TPC, the linear model had a higher predicted R^2 (0.9264) and lower PRESS (7.37) than the quadratic model (predicted R^2 = 0.8296; PRESS = 17.06). The added quadratic block was not significant ($p = 0.0714$). Nevertheless, lack-of-fit for the selected TPC model was significant ($p = 0.0426$). This result means that replicate variability at the center was smaller than the systematic residual variation across design points; high R^2 values therefore do not guarantee unbiased local predictions. The TPC model is appropriate for describing the dominant monotonic trend, especially the liquid-to-solid-ratio effect, but its point predictions particularly near boundaries must be treated cautiously. More design support, such as additional interior/axial points or a revised factor region, is required before claiming strong predictive validation.

For TFC, adding quadratic terms was not supported (sequential $p = 0.2077$) and sharply reduced predicted R^2 from 0.8148 to 0.5001. The selected linear model showed non-significant lack-of-fit ($p = 0.0636$), and adjusted and predicted R^2 differed by less than 0.2. The signal-to-noise ratios for both responses exceeded the recommended value of 4 [23]–[25].

The diagnostic plots are shown in Figure 1. Externally studentized residuals remained within ±3. Run 11 was influential for TPC (externally studentized residual = −2.785; Cook's distance = 0.557; DFFITS = −1.896), and run 3 was influential for TFC (−2.812; 0.563; −1.914, respectively). Both observations were retained because no documented experimental or transcription error was identified. Their influence, together with the small number of center replicates, reinforces the cautious interpretation of model predictions.

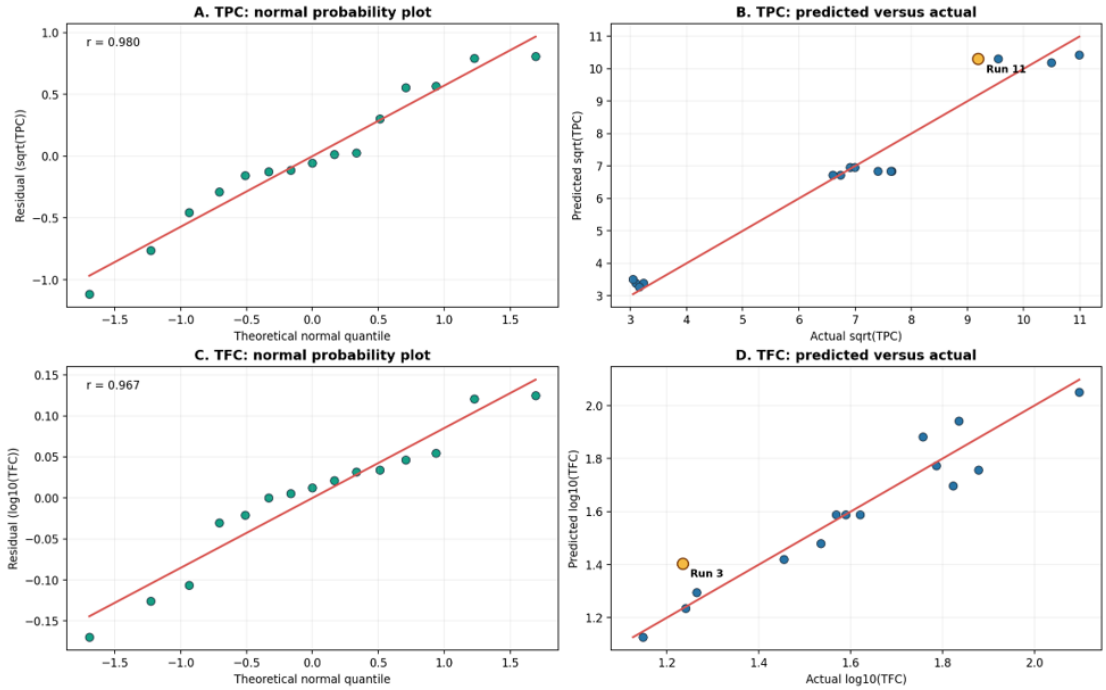

Figure 1 Residual and predicted-versus-actual diagnostics for the transformed TPC (A, B) and TFC (C, D) models. Influential runs retained in the analysis are highlighted.

3.2 Regression Equations and Factor Effects

The selected equations in actual factor units were:

Doi: 10.30872/jtpc.v10i2.430

$$\text{Sqrt(TPC)} = 1.24353 + 0.000015A + 0.230679B - 0.009498C \quad (1)$$

$$\log_{10}(\text{TFC}) = 0.951863 + 0.002890A + 0.021595B - 0.002373C \quad (2)$$

where A is ethanol concentration (%), B is liquid-to-solid ratio (mL/g), and C is extraction time (min). The equations predict the transformed responses. On the original scale, median TPC = [right-hand side of Eq. (1)]² and median TFC = 10^(right-hand side of Eq. (2)). Mean predictions require the bias corrections specified in Section 2.6.

For TPC, only B was significant ($p < 0.0001$); A ($p = 0.9973$) and C ($p = 0.5967$) were not. It is therefore not supported to describe ethanol concentration and time as dominant TPC determinants in this data set. The positive B coefficient is consistent with a larger concentration gradient and greater solvent capacity at higher liquid-to-solid ratios [26], [27]. The slight negative C coefficient is descriptive only and cannot be interpreted as evidence of time-dependent degradation because its effect was not significant.

For TFC, both A ($p = 0.0015$) and B ($p < 0.0001$) had significant positive effects, whereas C was not significant ($p = 0.3870$). The additive linear models contain no interaction terms, so the factor effects should not be described as synergistic. Figure 2 visualizes model-predicted TPC medians, and Figure 3 visualizes model-predicted TFC medians; each panel holds the third factor at its center value.

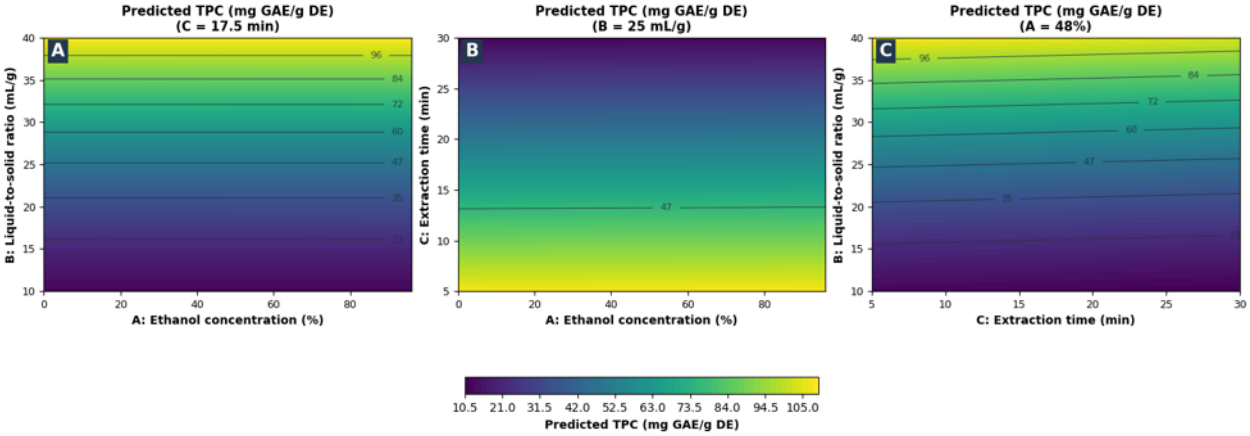

Figure 2 Model-predicted TPC medians across pairs of factors: (A) ethanol concentration and liquid-to-solid ratio at 17.5 min; (B) ethanol concentration and time at 25 mL/g; and (C) time and liquid-to-solid ratio at 48% ethanol.

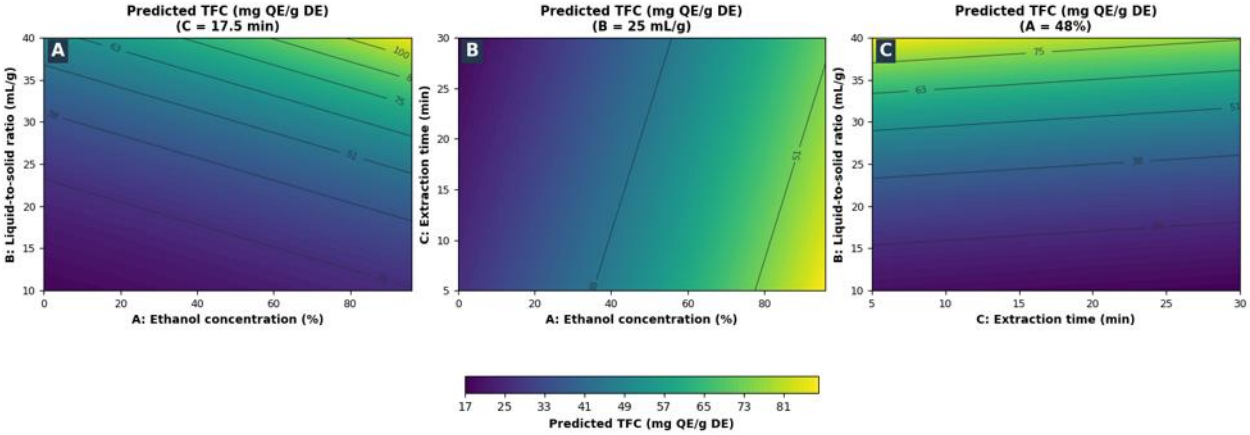

Figure 3 Model-predicted TFC medians across pairs of factors: (A) ethanol concentration and liquid-to-solid ratio at 17.5 min; (B) ethanol concentration and time at 25 mL/g; and (C) time and liquid-to-solid ratio at 48% ethanol. Units are mg QE/g DE.

Doi: 10.30872/jtpc.v10i2.430

3.3 Numerical Optimization and Independent Confirmation

With A, B, and C constrained to their study ranges and both responses set to maximize at equal importance, Design-Expert returned the leading solution at 95.994% ethanol, 40.000 mL/g, and 5.000 min (desirability = 0.955). The bias-corrected predicted means were 109.054 mg GAE/g DE for TPC and 123.371 mg QE/g DE for TFC; the corresponding predicted medians were 108.673 and 120.565 mg/g, respectively. Because this solution lies at or very near three factor limits and at an unsampled corner of the rectangular factor space, it should be regarded as a numerical model optimum requiring prospective experimental confirmation, not as a validated optimum.

An earlier confirmation experiment had been conducted at 82.8208% ethanol, 37.4455 mL/g, and 26.3205 min. This setting is distinct from the revised maximum-desirability solution and is therefore reported as an independent confirmation location rather than the final optimum. Triplicate results were 136.65 ± 3.16 mg GAE/g DE for TPC and 98.55 ± 0.01 mg QE/g DE for TFC. Table 3 compares these values with the corresponding model predictions.

Table 3 Model predictions and observed responses at the independent confirmation location (82.8208% ethanol, 37.4455 mL/g, 26.3205 min)

Response	Predicted mean	Predicted median	95% CI for mean	Observed mean ± SD (n = 3)	Absolute deviation/observed	Interpretation
TPC (mg GAE/g DE)	93.17	92.79	79.84–107.53	136.65 ± 3.16	31.82%	Observed mean outside CI; underprediction
TFC (mg QE/g DE)	88.59	86.57	68.98–113.76	98.55 ± 0.01	10.10%	Observed mean within CI

The marked TPC discrepancy is consistent with the significant lack-of-fit and shows that the TPC equation underestimated the response at this location. It cannot be attributed to a single demonstrated cause. Plausible contributors include residual curvature, run-to-run extraction variability, matrix heterogeneity, and analytical non-specificity. The Folin–Ciocalteu assay measures reducing capacity rather than phenolics exclusively; reducing sugars, ascorbic acid, and other reductants can elevate apparent TPC [28], [29]. Such compounds may be co-extracted from M. charantia, particularly at high liquid-to-solid ratio. This is a mechanistic possibility, not proof that interference caused the observed difference, because no matrix clean-up or compound-specific analysis was performed.

In contrast, the TFC confirmation mean was within the model's 95% confidence interval and differed from the predicted mean by 10.10%. This supports cautious use of the TFC model within the studied region, although the small experimental design and influential observation still limit broad generalization.

3.4 Process Implications and Limitations

The nominal rated-power density of the 2 L bath was 60 W/L. This value facilitates equipment description but is not equivalent to measured acoustic intensity or absorbed power. Industrial translation would require calorimetric or hydrophone-based characterization, control of vessel position and bath loading, and comparison on the basis of acoustic energy density or specific energy. Scale-up studies demonstrate that frequency, intensity, amplitude, flow configuration, and energy input must be matched to geometry rather than transferred from nominal wattage alone [17], [18].

Four limitations define the scope of the conclusions. First, temperature was fixed at 50 °C and therefore was controlled rather than optimized. Second, ultrasound frequency and power were fixed and actual acoustic power was not measured. Third, the Folin–Ciocalteu result represents total reducing capacity and may include non-phenolic interferents. Fourth, the TPC model had significant lack-of-fit and the revised numerical optimum is at an unsampled boundary corner without prospective confirmation. Future work should add design points around the proposed optimum, include temperature and measured acoustic energy as factors, increase replication, and verify phenolics by an assay incorporating clean-up or compound-specific chromatography.

Doi: 10.30872/jtpc.v10i2.430

4 Conclusion

Square-root-transformed TPC and $\log_{10}$-transformed TFC were described by parsimonious linear models across the studied BBD. The liquid-to-solid ratio was the only significant TPC factor, whereas ethanol concentration and liquid-to-solid ratio significantly affected TFC; extraction time was not significant for either response. Joint numerical optimization predicted 95.994% ethanol, 40.000 mL/g, and 5.000 min (desirability 0.955), with mean responses of 109.054 mg GAE/g DE and 123.371 mg QE/g DE. This boundary solution has not been experimentally confirmed. The TFC model showed non-significant lack-of-fit and reasonable agreement at an independent confirmation location, whereas the significant TPC lack-of-fit and substantial underprediction show that the TPC model requires refinement before confirmatory or scale-up use. The study therefore provides a preliminary model-guided operating direction rather than a fully validated industrial optimum.

5 Declarations

5.1 Acknowledgements

This research was funded by Ministry of Research, Technology and Higher Education Indonesia (Grant No. 101/SPK/D.D4/PPK.01.APTV/III/2024 and Grant No. 001/SP2H/RT-MONO/LL4/2024).

5.2 Author contributions

Tubagus Akmal: Conceptualization, methodology, experimental design, software, formal analysis, data interpretation, visualization, writing original draft, writing review and editing, supervision, project administration, and funding acquisition. Cszahreyloren Vitamia: Investigation, laboratory experiments, data collection, data curation, and manuscript revision. Andi Ika Julianti Handayani: Methodology, validation, interpretation of results, writing review and editing, and supervision. All authors have read and approved the final version of the manuscript.

5.3 Conflict of Interest

The authors declare that they have no conflicts of interest related to this study.

5.4 Funding Statement

The funders had no role in study design, data collection, analysis, interpretation, manuscript preparation, or the decision to submit the article.

6 Bibliography

[1] S. Sur and R. B. Ray, "Bitter melon (Momordica charantia), a nutraceutical approach for cancer prevention and therapy," *Cancers (Basel).*, vol. 12, no. 8, pp. 1–22, 2020, doi: 10.3390/cancers12082064.

[2] M. Muronga *et al.*, "Three Selected Edible Crops of the Genus Momordica as Potential Sources of Phytochemicals: Biochemical, Nutritional, and Medicinal Values," *Front. Pharmacol.*, vol. 12, no. May, pp. 1–19, 2021, doi: 10.3389/fphar.2021.625546.

[3] T. Akmal and L. Sasongko, "INFLUENCE OF Momordica charantia (L.) ON THE PHARMACOKINETICS AND PHARMACODYNAMICS OF GLICLAZIDE IN ALLOXAN-INDUCED DIABETIC RATS," *Med. Sains J. Ilm. Kefarmasian*, vol. 8, no. 3, pp. 1079–1088, 2023, doi: 10.37874/ms.v8i3.854.

[4] O. Zannou, H. Pashazadeh, M. Ghellam, A. Ali Redha, and I. Koca, "Enhanced ultrasonically assisted extraction of bitter melon (Momordica charantia) leaf phenolic compounds using choline chloride-acetic acid–based natural deep eutectic solvent: an optimization approach and in vitro digestion," *Biomass Convers. Biorefinery*, vol. 14, no. 10, pp. 11491–11503, 2024, doi: 10.1007/s13399-022-03146-0.

[5] Z. Wang, S. Li, S. Ge, and S. Lin, "Review of Distribution, Extraction Methods, and Health Benefits of Bound Phenolics in Food Plants," *J. Agric. Food Chem.*, vol. 68, no. 11, pp. 3330–3343, 2020, doi: 10.1021/acs.jafc.9b06574.

[6] J. Liu, Y. Guo, J. Sun, Y. Lei, M. Guo, and L. Wang, "Extraction methods, multiple biological

activities, and related mechanisms of Momordica charantia polysaccharide: A review," *Int. J. Biol. Macromol.*, vol. 263, no. P2, p. 130473, 2024, doi: 10.1016/j.ijbiomac.2024.130473.

[7] E. Quitério, C. Grosso, R. Ferraz, C. Delerue-Matos, and C. Soares, "A Critical Comparison of the Advanced Extraction Techniques Applied to Obtain Health-Promoting Compounds from Seaweeds," *Mar. Drugs*, vol. 20, no. 11, pp. 1–40, 2022, doi: 10.3390/md20110677.

[8] T. Akmal, Y. P. Tanjung, A. I. Julianti, and A. G. Lestari, "Influence of extraction method on total phenolic content and antioxidant activity of Sappan Wood (Caesalpinia sappan L.) extract," *Sasambo J. Pharm.*, vol. 5, no. 2, pp. 55–62, 2024, doi: https://doi.org/10.29303/sjp.v5i2.364.

[9] T. Akmal, A. I. Julianti, Y. P. Tanjung, P. Mutiara, and S. Febriyanti, "Effect of extraction method on total phenolic content and antioxidant activity of Terminalia catappa (L .) leaves The impact of technological advancements on human beings is not always," *PHARMASIPHA Pharm. J. Islam. Pharm.*, vol. 8, no. 2, pp. 1–11, 2024.

[10] L. Shen *et al.*, "A comprehensive review of ultrasonic assisted extraction (UAE) for bioactive components: Principles, advantages, equipment, and combined technologies," *Ultrason. Sonochem.*, vol. 101, no. October, p. 106646, 2023, doi: 10.1016/j.ultsonch.2023.106646.

[11] K. Kumar, S. Srivastav, and V. S. Sharanagat, "Ultrasound assisted extraction (UAE) of bioactive compounds from fruit and vegetable processing by-products: A review," *Ultrason. Sonochem.*, vol. 70, no. July 2020, p. 105325, 2021, doi: 10.1016/j.ultsonch.2020.105325.

[12] Y. Xiang, Z. Liu, Y. Liu, B. Dong, C. Yang, and H. Li, "Ultrasound-assisted extraction, optimization, and purification of total flavonoids from Daphnegenkwa and analysis of their antioxidant, anti-inflammatory, and analgesic activities," *Ultrason. Sonochem.*, vol. 111, no. September, p. 107079, 2024, doi: 10.1016/j.ultsonch.2024.107079.

[13] A. Sanou *et al.*, "Modelling and optimisation of ultrasound-assisted extraction of roselle phenolic compounds using the surface response method," *Sci. Rep.*, vol. 13, no. 1, pp. 1–9, 2023, doi: 10.1038/s41598-023-27434-5.

[14] I. A. Almusallam *et al.*, "Optimization of ultrasound-assisted extraction of bioactive properties from date palm (Phoenix dactylifera L .) spikelets using response surface methodology," *LWT*, vol. 140, no. December 2020, p. 110816, 2021, doi: 10.1016/j.lwt.2020.110816.

[15] N. M. Hani, A. E. Torkamani, S. Zainul Abidin, W. A. K. Mahmood, and P. Juliano, "The effects of ultrasound assisted extraction on antioxidative activity of polyphenolics obtained from Momordica charantia fruit using response surface approach," *Food Biosci.*, vol. 17, pp. 7–16, 2017, doi: https://doi.org/10.1016/j.fbio.2016.11.002.

[16] J. J. Lee and K. Y. Yoon, "Optimization of ultrasound-assisted extraction of phenolic compounds from bitter melon (Momordica charantia) using response surface methodology," *CyTA - J. Food*, vol. 19, no. 1, pp. 721–728, Jan. 2021, doi: 10.1080/19476337.2021.1973110.

[17] Y. Tao, Z. Zhang, and D.-W. Sun, "Kinetic modeling of ultrasound-assisted extraction of phenolic compounds from grape marc: Influence of acoustic energy density and temperature," *Ultrason. Sonochem.*, vol. 21, no. 4, pp. 1461–1469, 2014, doi: https://doi.org/10.1016/j.ultsonch.2014.01.029.

[18] Ó. Rodríguez, S. Bona, A. Stäbler, and L. Rodríguez-Turienzo, "Ultrasound-Assisted Extraction of Polyphenols from Olive Pomace: Scale Up from Laboratory to Pilot Scenario," *Processes*, vol. 10, no. 12. p. 2481, 2022. doi: 10.3390/pr10122481.

[19] T. Akmal, A. I. Julianti, and S. S. Syamsudin, "Polyherbal Formulation Optimization From Clitoria Ternatea, Rosmarinus Officinalis and Aquilaria Malaccensis Using Simplex Lattice Design," *Int. J. Appl. Pharm.*, vol. 15, no. Special Issue 2, pp. 79–84, 2023, doi: 10.22159/ijap.2023.v15s2.15.

[20] F. Jasmin, A. Ika, J. Handayani, T. Akmal, B. Siliwangi, and P. Academy, "Optimization of Extraction Parameters for Phenolics and Flavonoids from Peony (Paeonia lactiflora) Flowers Using Ultrasound-Assisted Extraction," *Hydrog. J. Kependidikan Kim.*, vol. 13, no. 1, pp. 1–11, 2025, doi: https://doi.org/10.33394/hjkk.v13i1.14346.

Doi: 10.30872/jtpc.v10i2.430

[21] D. Ananda, A. I. Julianti, and T. Akmal, "Optimization of Phenolic and Flavonoid Extraction in Lavandula Angustifolia using Ultrasonic Assistance Extraction," *Reka Buana J. Ilm. Tek. Sipil dan Tek. Kim.*, vol. 10, no. 1, pp. 25–36, 2025, doi: https://doi.org/10.33366/rekabuana.v10i1.6608 keywords:

[22] L. M. Anaya-Esparza *et al.*, "Design of Experiments for Optimizing Ultrasound-Assisted Extraction of Bioactive Compounds from Plant-Based Sources," *Molecules*, vol. 28, no. 23. p. 7752, 2023. doi: 10.3390/molecules28237752.

[23] O. By-products, R. Quirantes-piné, and J. Lozano-sánchez, "Optimized Ultrasound-Assisted Extraction for Enhanced Recovery of Valuable Phenolic Compounds from," *Antioxidants*, no. 14, p. 938, 2025, doi: https://doi.org/10.3390/ antiox14080938.

[24] A. A. Bin, A. Hamid, and K. Kerboua, "Ultrasonics Sonochemistry Ultrasonic-assisted extraction to enhance the recovery of bioactive phenolic compounds from Commiphora gileadensis leaves," *Ultrason. Sonochem.*, vol. 105, no. December 2023, p. 106852, 2024, doi: 10.1016/j.ultsonch.2024.106852.

[25] D. Hu, R. Xue, X. Zhuang, and X. Zhang, "Ultrasound-assisted extraction optimization of polyphenols from Boletus bicolor and evaluation of its antioxidant activity," *Front. Nutr.*, no. March, pp. 1–14, 2023, doi: 10.3389/fnut.2023.1135712.

[26] S. Sai-Ut, P. Kingwascharapong, M. A. Mazumder, and S. Rawdkuen, "Optimization of Ethanolic Extraction of Phenolic Antioxidants from Lychee and Longan Seeds Using Response Surface Methodology," *Foods*, vol. 12, no. 15. p. 2827, 2023. doi: 10.3390/foods12152827.

[27] A. C. Andrade, F. T. Borsoi, A. S. Saliba, S. M. de Alencar, G. M. Pastore, and H. S. Arruda, "Optimization of Ultrasonic-Assisted Extraction of Phenolic Compounds and Antioxidant Activity from Araticum Peel Using Response Surface Methodology," *Plants*, vol. 13, no. 18. p. 2560, 2024. doi: 10.3390/plants13182560.

[28] J. Pico, R. Y. Pismag, M. Laudouze, and M. M. Martinez, "Systematic evaluation of the Folin–Ciocalteu and Fast Blue BB reactions during the analysis of total phenolics in legumes, nuts and plant seeds," *Food Funct.*, vol. 11, no. 11, pp. 9868–9880, Nov. 2020, doi: 10.1039/d0fo01857k.

[29] I. L. Lawag, E. S. Nolden, A. A. M. Schaper, L. Y. Lim, and C. Locher, "A Modified Folin-Ciocalteu Assay for the Determination of Total Phenolics Content in Honey," *Applied Sciences*, vol. 13, no. 4. p. 2135, 2023. doi: 10.3390/app13042135.

[30] S. Niglio, C. Razola-díaz, H. Waegeman, and V. Verardo, "Food grade pilot scale strategy for non-thermal extraction and recovery of phenolic compounds from orange peels," *LWT*, vol. 205, no. June, p. 116538, 2024, doi: 10.1016/j.lwt.2024.116538.

[31] Y. Zhou and D. Lin, "Ultrasound-assisted optimized extraction and analysis of polysaccharides of Tricholoma matsutake," no. September, pp. 1–11, 2024, doi: 10.3389/fsufs.2024.1433565.